

OUTPUT FILTER SIZING OF GRID CONNECTED BUCK-BOOST INVERTER USING GRAPHICAL APPROACH

Dedet Candra Riawan¹, Sjamsjul Anam², and Heri Suryoatmojo³

^{1,2,3}Electrical Engineering Department, Institut Teknologi Sepuluh Nopember, Kampus ITS Sukolilo, Surabaya, Indonesia, e-mail: dedet.riawan@ee.its.ac.id

Received Date: May 4, 2016

Abstract

Wide range input voltage converters are merely required in photovoltaic and wind energy conversion systems which have dynamic output voltage due to irradiance and wind speed fluctuations. This paper presents a comprehensive analysis and design approach of grid connected buck-boost inverter for wide input voltage application. Sizing of a LC output filter component is emphasized in this paper. It is important to size the filter properly to obtain a trade-off between output current ripple and reactive power supplied into grid when inverter is in stand-by mode. A graphical method is employed to determine filter parameters. The presented method is found to be straight forward and easy from practical point of view.

Keywords: Buck-boost inverter, Filter sizing, Graphical approach

Introduction

Several on-grid converter configurations have been proposed for photovoltaic and variable speed wind turbine generator applications. The most common method is using ac-dc-ac (asynchronous) link[1]–[3]. The main elements in this configuration are rectifier, dc bus and inverter. Rectifier can be either an uncontrolled or a controlled type. Pulse Width Modulated Current-controlled Voltage Source Inverter (PWM CCVSI) is used to control power flow from dc bus to the grid. In this configuration dc bus voltage level must be kept above peak value of grid voltage to maintain inverter works. Therefore, a boost dc-dc converter is often included between rectifier and inverter.

Two CCVSI's in back-to-back configuration offers better performance[4], [5] in variable speed application such as in Self-Excited Induction Generator (SEIG) systems as the machine side inverter replaces the rectifier providing excitation control of the SEIG, while the grid side inverter controls power flow from dc bus to the grid. As a result, wider speed range of SEIG is achieved. However, this configuration costs the overall system more than an asynchronous link at the same power rating because two full-sized inverters must be used. To improve waveform quality of inverter, multi level inverters with advance switching technique have been introduced[6], [7]. Some topology offer switching device reduction which results in less complexity of control[8].

Matrix converter is another converter configuration that suits variable speed operation[9], [10]. Its advantages over the conventional back-to-back PWM inverter include retaining its conventional configurations such as bidirectional power flow and independent voltage control without the need for the bulky dc capacitor.

Buck-boost inverter is widely used in small PV generation system[11], [12] because of its wide range input voltage. This paper presents a comprehensive analysis and design of single phase buck-boost inverter topology, in which new graphical approach is employed to determine the size of filter component.

Figure 1 shows overall power stage and control diagrams of the studied converter system. The power stage comprises buck-boost converter and grid switcher while the main control part elements are modulator and feed-forward power control strategy.

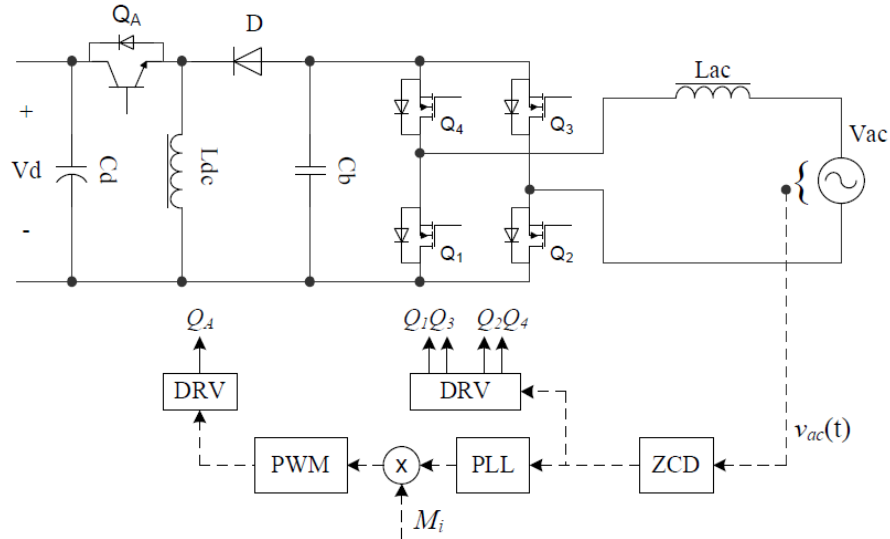


Figure 1. Diagram of buck-boost inverter with grid interface capability.

Analysis of Buck-Boost Inverter Feeding Grid

Buck-Boost Inverter Operation Principles

As shown in Figure 1, the inverter configuration has two stages, i.e. buck-boost and full bridge converters. A conventional buck-boost converter is used in this inverter configuration to utilize its step-up and step-down properties. Buck-boost converter operates as a current source which generates absolute sinusoidal current from the dc voltage source. At the grid side a full bridge converter operates in current source mode to interface buck-boost output and grid. Figure 2 shows the principle of the inverter operation in their corresponding waveforms.

The advantage of topology shown in Figure 1 is only switch Q_A is modulated in high frequency PWM. This simplifies the control of power flow and wave shaping in the inverter. Full bridge inverter switches ($Q_1 - Q_4$) are switched to follow the phase angle of grid voltage. Switching loss is almost non-existent at this stage because grid voltage magnitude is normally zero at the zero-crossing vicinity. Also, the control topology allows the inverter to have an almost unity power factor because the current modulated by buck-boost is kept in phase with grid voltage by phase-locked loop (PLL).

Buck-boost stage in this topology is designed to operate in discontinuous conduction mode (DCM) with absolute sine modulation signal written as:

$$D(t) = M_i \times |\sin(\omega t)| \quad (1)$$

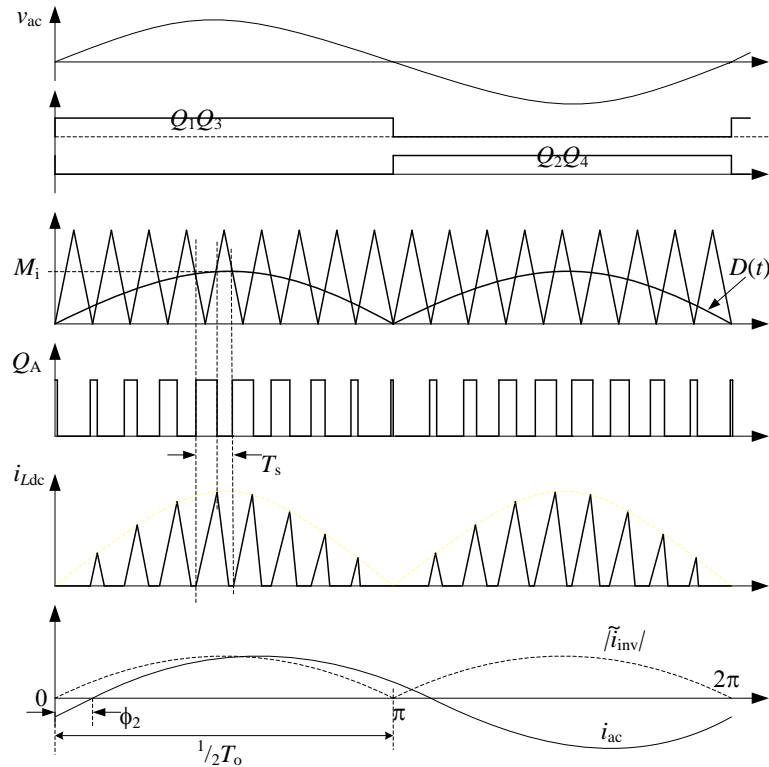


Figure 2. Key waveforms of buck-boost inverter. From top to the bottom: grid voltage, full-bridge gate signals, modulation & carrier signals, buck-boost gate signal, inductor current, ac side current.

Modulation signal has a magnitude of M_i that represents depth of modulation (modulation index) of the inverter as shown in Figure 2. Depth of modulation controls the power from dc voltage source to the output that can be expressed as:

$$\begin{aligned}
 P_d &= \frac{1}{\frac{1}{2}T_o} \int_0^{\frac{1}{2}T_o} \frac{1}{2} \frac{V_d^2}{L_{dc}} \frac{d(t)^2}{f_s} dt \\
 &= \frac{1}{\pi} \int_0^{\pi} \left[\frac{1}{2} \frac{V_d^2}{L_{dc}} \frac{(M_i \sin(\omega t))^2}{f_s} \right] d(\omega t) \\
 &= \frac{1}{4} \frac{V_d^2}{L_{dc}} \frac{M_i^2}{f_s}
 \end{aligned} \tag{2}$$

In order to maintain DCM operation of buck-boost converter, depth of modulation must be below a certain value that depends on input and output voltage. Otherwise, converter will operate in continuous conduction mode which is avoided in this topology. Limitation on depth of modulation index can be written in term of input and grid voltages as:

$$M_{i(\max)} = \frac{\sqrt{2}V_{ac}}{\sqrt{2}V_{ac} + V_d} \tag{3}$$

P_d	dc input power (Watt)
V_d	dc input voltage (Volt-dc)
V_{ac}	ac grid voltage (Volt-rms)
M_i	depth of modulation
L_{dc}	buck-boost inductor (Henry)
f_s	buck-boost switching frequency (Hertz)

Equations in (2) can be used to calculate inductor value L_{dc} for given input and output voltages. In this analysis, output voltage is assumed constant which is provided by strong grid. Substituting maximum value of modulation index (3) into (2) will result in power limitation on the inverter. The limitation is a useful measure to determine the range of input voltage especially when the generated power by voltage source is dependent on voltage such as in photovoltaic and variable speed wind turbine generation systems.

Inverter input power control can be achieved by adjusting depth of modulation based on input voltage level. Such technique offers not only fast response but also stable control which is the nature of feed forward control.

Output Filter Sizing and Ripple Analysis

When buck-boost inverter is connected to the grid through a filter, its performance (power factor and current ripple) is determined by output filter elements indicated as C_b and L_{ac} in equivalent circuit shown in Figure 3a. Note that C_b is actually buck-boost output filter as described in Figure 1. Fundamental frequency is used to analyze voltage and current since high frequency ripple component is suppressed completely. Analysis begins with current equation in phasor representation derived from equivalent circuit in Figure 3b.

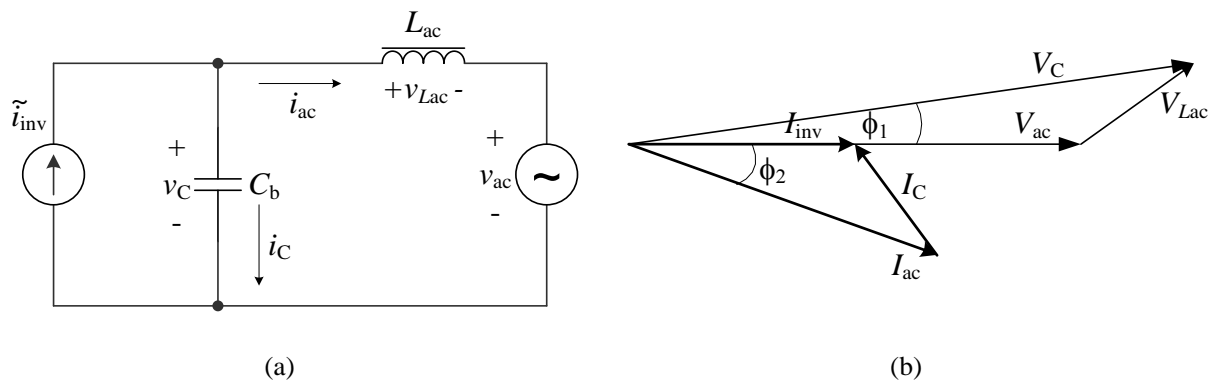


Figure 3. (a)Equivalent circuit of inverter with filter elements and (b) phasor diagram

Applying super-position method on the equivalent circuit for I_{ac} will result in inverter current and grid voltage that can be written as:

$$\vec{I}_{ac} = -\underbrace{\frac{\vec{I}_{inv}}{\omega^2 L_{ac} C_b - 1}}_{\text{Re}} + j \underbrace{\frac{\vec{V}_{ac}}{\omega L_{ac} - \frac{1}{\omega C_b}}}_{\text{Im}} \quad (4)$$

V_{ac}	grid voltage (in phasor)
I_{inv}	inverter output current (averaged in phasor)
L_{ac}	output filter inductor
C_b	buck-boost output filter capacitor (brought to ac side)
ω	angular frequency of grid voltage

Power factor of inverter can be represented as ϕ_1 which is defined as phase different between inverter voltage V_C and inverter current I_{inv} . In practical, power factor is seen from grid side. Therefore it is preferred to define phase different between grid voltage V_{ac} and grid current I_{ac} as the actual power factor of the system. Actual power factor is denoted by phase angle ϕ_2 in Figure 3b. In this analysis inverter current and grid voltage were chosen to have zero phase angles due to PLL described in Figure 1. Thus, phase angle can be obtained from (4) by analyzing real and imaginary part of I_{ac} .

$$\phi_2 = \tan^{-1} \left(\frac{\text{Im}(\vec{I}_{ac})}{\text{Re}(\vec{I}_{ac})} \right) \quad (5)$$

Imaginary part of I_{ac} is easily obtained from (4) as

$$\text{Im}(\vec{I}_{ac}) = \frac{\vec{V}_{ac}}{\omega L_{ac} - \frac{1}{\omega C_b}} = \frac{\sqrt{2}V_{ac}\omega C_b}{\omega^2 L_{ac} C_b - 1} \quad (6)$$

Real part of grid current I_{ac} can be obtained more easily from power equation instead from (4). Output power delivered into grid P_{ac} is simply written as:

$$P_{ac} = V_{ac} \underbrace{I_{ac} \cos \phi_2}_{\frac{1}{\sqrt{2}} \text{Re}(\vec{I}_{ac})} \quad \text{Thus, } \text{Re}(\vec{I}_{ac}) = \frac{\sqrt{2}P_{ac}}{V_{ac}} \quad (7)$$

V_{ac} is rms value of grid voltage. Substituting (6) and (7) into (5) yields more informative expression of phase angle in term of power and grid voltage which can be written as:

$$\phi_2 = \tan^{-1} \left(\frac{\omega C_b V_{ac}^2}{P_{ac} (\omega^2 L_{ac} C_b - 1)} \right) \quad (8)$$

Note that phase angle in (8) is seen as leading power factor from grid point of view because grid is considered as load by inverter grid-feeding scheme. According to (8), power factor varies along with output power when filter component and grid voltage are constants. Expression in (8) can be used to calculate the value of filter component at a specified output power and power factor.

However, expression in (8) does not provide output current ripple information which is important in converter design. Current ripple at output due to high switching frequency can be analyzed using equivalent circuit shown in Figure 4a. If grid voltage is purely sinusoidal, all harmonic components of voltage will appear at inductor as ripple.

In most high frequency switching converter, voltage ripple across capacitor can be approximated by triangular waveform to reduce complexity of the analysis (Figure 4b). Thus, current ripple flowing in the inductor L_{ac} can be calculated as follow.

$$i_{ac-rip} = \frac{v_{inv-rip}}{X_{L_{ac}}} = \frac{v_{inv-rip(p)} / \sqrt{3}}{\omega_s L_{ac}} \quad (9)$$

$$= \frac{\Delta v_{C(pp)}}{4\sqrt{3}\pi f_s L_{ac}}$$

Maximum peak value of voltage across capacitor C_b is obtained from switching cycle analysis of buck-boost converter at the boundary between continuous conduction mode (CCM) and DCM operations in (2) and (3) as:

$$\Delta v_{C(pp)} = \frac{1}{2} \frac{\left(\frac{V_d M_{i(max)}}{L_{dc} f_s} - \sqrt{2} I_{ac} \right)^2 L_{dc}}{\sqrt{2} V_{ac} C_b} \quad (10)$$

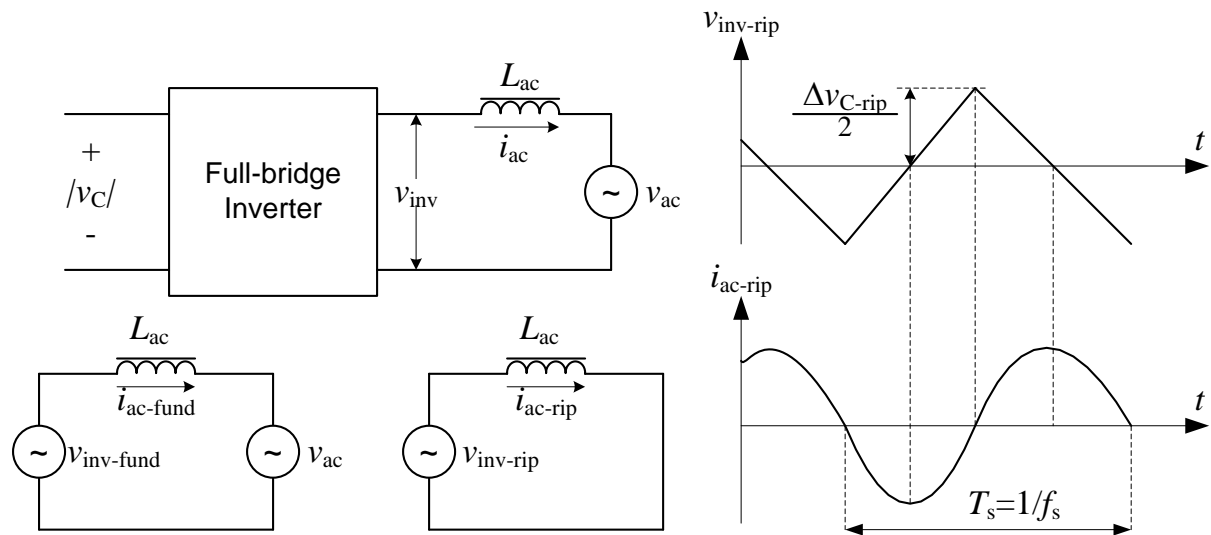


Figure 4. (a) Equivalent circuit of filter considering harmonics components and (b) ripple waveforms.

At this point, filter inductor L_{ac} and filter capacitor C_b can be calculated using (8) to (10) at specified output power, power factor, and output current ripple. Graphical method is found to be a useful method when several mathematical expressions are involved. Graphical method was developed to determine minimum inductor and capacitor requirement, which is shown in next section.

Design, Simulation and Experimental Results

This section presents steps in buck-boost inverter design and how the graphical method will used to determine filter element C_b and L_{ac} . First step is determining buck-boost

inductor L_{dc} for a given nominal output power and input voltage. The calculated inductance is then used to determine filter element by utilizing developed graphic inspection.

Design Calculation

The inverter is designed to have a wide input voltage range from 150 Vdc to 400 Vdc. Specification of inverter for design is listed in detail in Table I. Switching frequency of 15625 Hz for buck-boost stage is intentionally chosen to suit 8-bit microcontroller in hardware implementation. For a given switching frequency, maximum value of buck-boost inductor L_{dc} can be calculated using (2) and (3) as:

$$L_{dc} \leq \frac{\left(\frac{240\sqrt{2}}{240\sqrt{2} + 400} \right)^2 \times 400^2}{4 \times 2000 \times 15625} \approx 270 \mu H$$

Lower inductance value of 250 μH is chosen in design to avoid CCM operation due to tolerance of practical component.

Table I. Inverter Design Specification

Parameter	Notation	Value
Output power	P_o	2.0 kW
Input voltage	V_d	100 Vdc to 400 Vdc
Output voltage	V_{ac}	240 Vac, 50 Hz
Power factor	pf	> 0.99 at rated power
Output current ripple	I_{ac-rip}	<2% of rated

Buck-boost dc filter capacitor C_b can be determined using (8) by varying the value of L_{ac} for a given output power, power factor, and grid voltage. Once correlation between C_b and L_{ac} is obtained, output current ripple in L_{ac} can be calculated using (9) and (10). Graphical method in Figure 5 shows the variation of buck-boost dc filter capacitor and output current ripple when output filter inductor L_{ac} varies from 100 μH to 2 mH. Output current ripple is used as the constraint in the design which is set to be less than 2% from its full load current. Graphical inspection shows that an inductor of 320 μH is the lowest value to meet output current ripple requirement. Higher value may be used due to tolerance of inductance value in practical inductor. In this design a 400 μH inductor is chosen.

Applying same method, maximum capacitance of C_b of 15.47 μF should be used to keep high power factor in the inverter. However, capacitance of C_b does not change significantly against inductor as seen in the graph. Therefore, a 15 μF capacitor would be sufficient to keep high power factor at grid side.

Simulation Result

Simulation of the buck-boost inverter is performed using computer simulation by assuming all elements are ideal components including input voltage source and grid voltage. Switches Q_1 - Q_4 are controlled by a zero crossing detector measured from the grid voltage. Switch Q_A is modulated in high frequency PWM generated by triangular and sine waveforms. Gate signals of the buck-boost and full-bridge stages are shown in Figure 6.

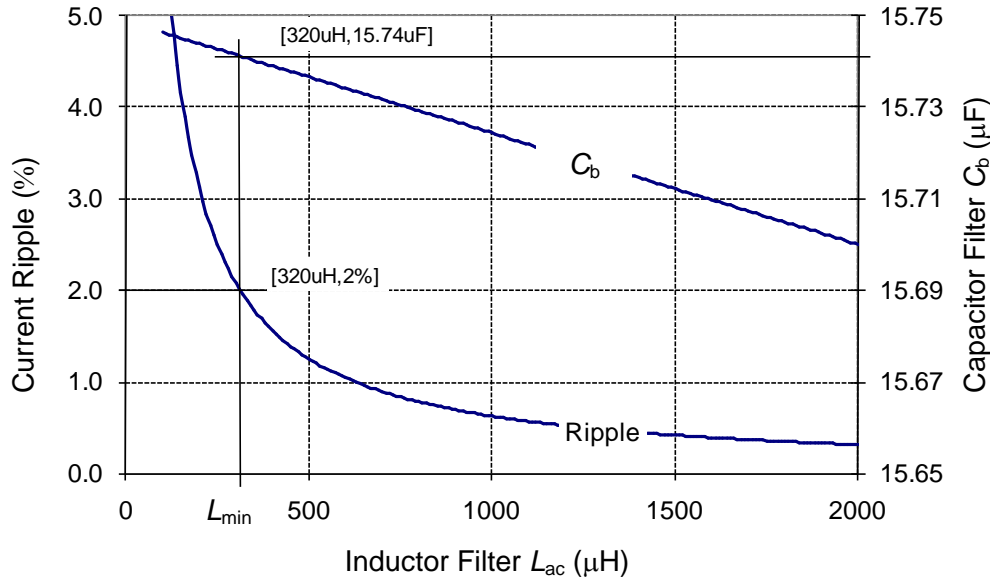


Figure 5. Graphical method for filter element sizing, C_b and L_{ac} .

Figure 7 shows capacitor voltage and inductor current with grid voltage as the reference for buck-boost stage. Capacitor voltage contains ripple as predicted in the previous analysis. The peak to peak voltage ripple obtained from simulation is 25.6 Volts which has good conformity with the theoretical value calculated using (10). Further filtering by the inductor suppresses output current ripple to 0.476 Amperes (peak to peak). This ripple is just below 2% which satisfies the design requirement.

Waveform of the inverter output current injected into the grid is shown in Figure 8, which also shows detail of the ripple component of the output current. Phase shift between grid voltage and current is inevitable in a buck-boost inverter due to the nature of the filter elements. The output current shown in Figure 8 has a phase shift of 8.6° which corresponds to a 0.988 power factor. This power factor is seen as “leading by grid” which means reactive power is being injected into the grid. The amount of reactive power generated by the inverter can be calculated as:

$$Q_{ac} = V_{ac} I_{ac} \sin \phi_2 = 240 \times 8.35 \times 0.988 = 300 \text{ VAR}$$

This reactive power is constant at a wide range of output power values because of the presence of C_b across grid terminal all the time. The inverter always supplies reactive power to the grid even when the inverter is not generating active power. Therefore, it is preferred to use small filter capacitor to maintain low reactive power injection to grid.

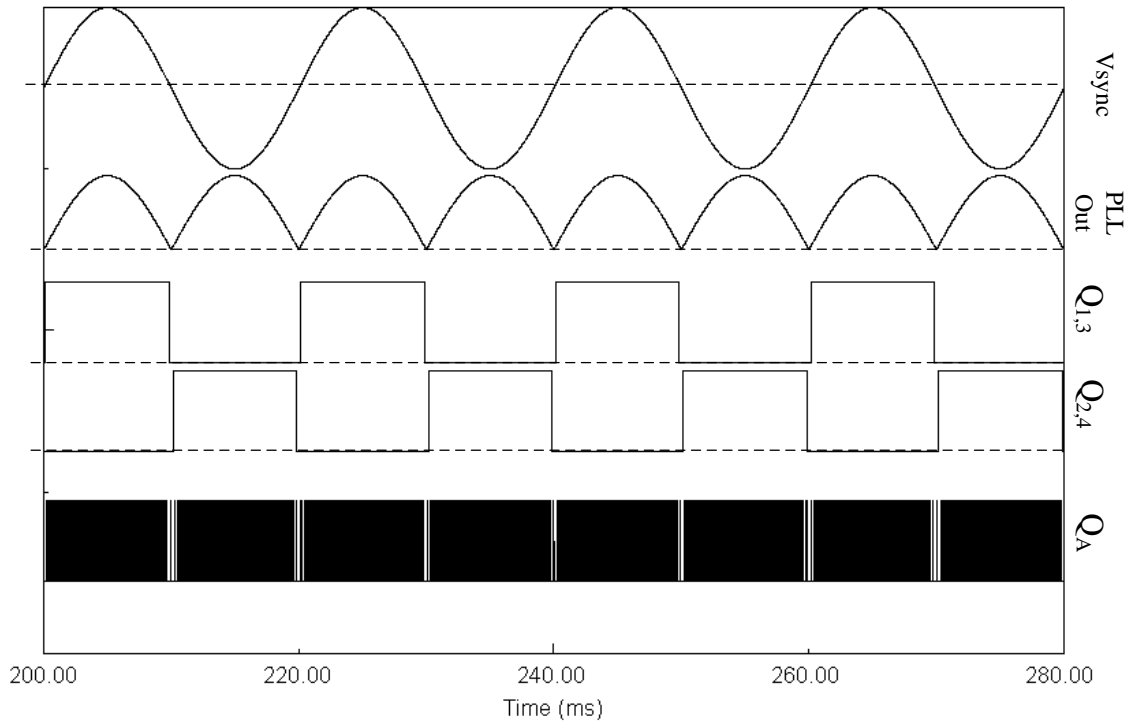


Figure 6. Control waveforms of simulated buck-boost inverter.

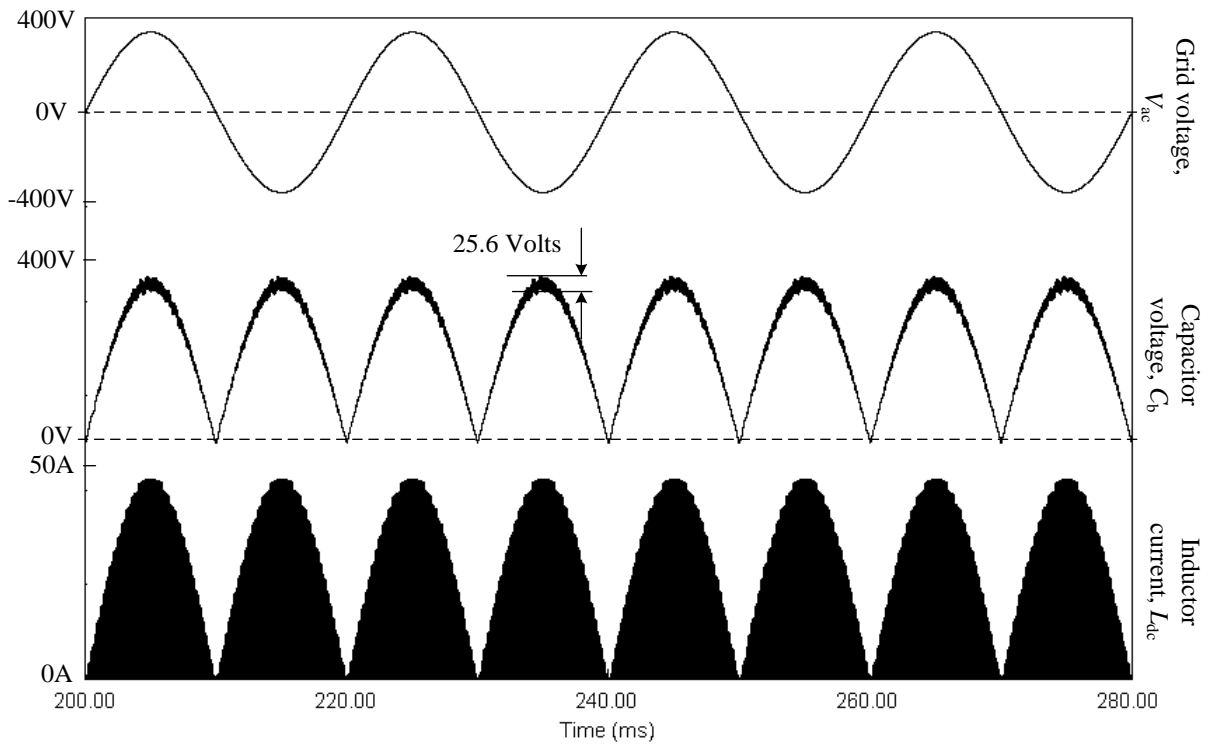


Figure 7. Simulated grid voltage, capacitor voltage and dc inductor current at full load.

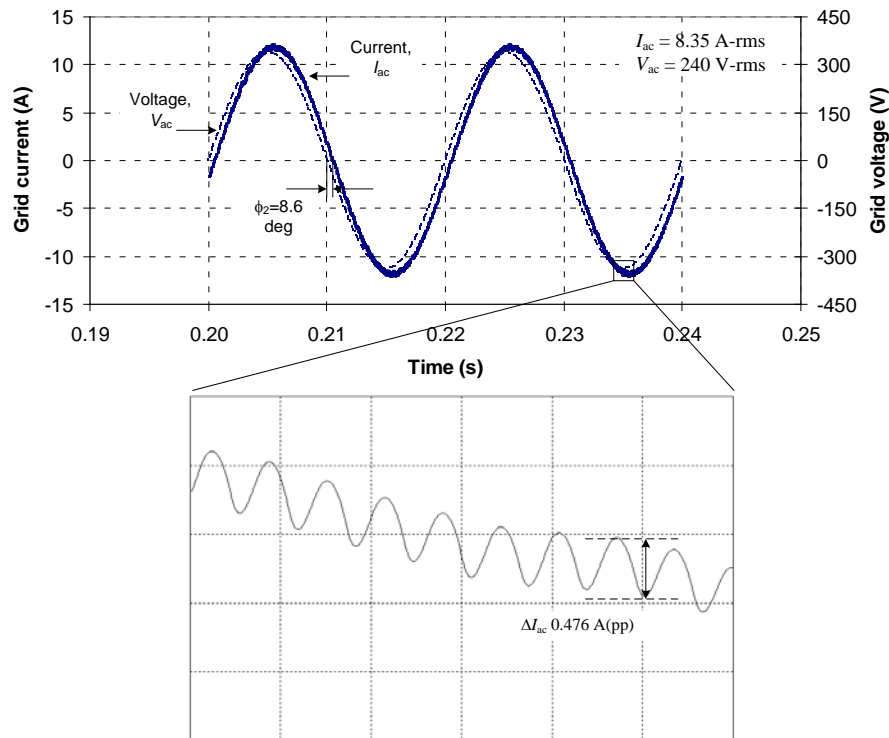


Figure 8. Simulated output current and grid voltage at full load. Inset: current ripple.

Experimental Result

A scaled-down prototype of the inverter has been built to verify theoretical and simulation results. Power stage of the inverter is rated at 1 kVA with input voltage range from 40 - 200 Volts dc and grid voltage of 120 Volts ac. The value of L_{dc} , C_b and L_{ac} are 110 μH , 30 μF , and 500 μH respectively. A 1.5 kVA commercial inverter was used to generate pure sine waveform simulating grid voltage at 120 Volts ac as shown in Figure 9. For control circuits, low cost 8-bit microcontrollers were used to implement PLL, modulator, and power control. Figure 10 shows a photograph of the developed buck-boost inverter and its control.

Test is performed to investigate the waveforms generated by both control and power circuits of the inverter. Inverter input voltage is set to 100 Volt dc while output voltage is 120 Volts ac. Captured waveforms are shown from Figure 11 to Figure 13. The gate signals on switches Q_A and Q_1 to Q_4 are shown in Figure 11 with the grid voltage as a reference. Figure 12 gives a picture of inverter power stage waveforms, i.e. grid voltage, dc bus voltage, output current and inductor current. Those waveforms are taken in boost mode at which the magnitude of the input voltage is lower than the peak value of the grid voltage. Ripples on the output current caused by high frequency switching are shown in detail in Figure 13, along with inductor current Q_A , gate signal and voltage across buck-boost switch V_{QA} . Measured ripple on the output current is 0.384 Amperes (peak to peak) which corresponds to 3.25% of inverter peak current. Detailed waveforms are measured at the peak of grid voltage where the duty cycle reached its maximum value. It can be noticed that inductor current is maintained at discontinuous operation.

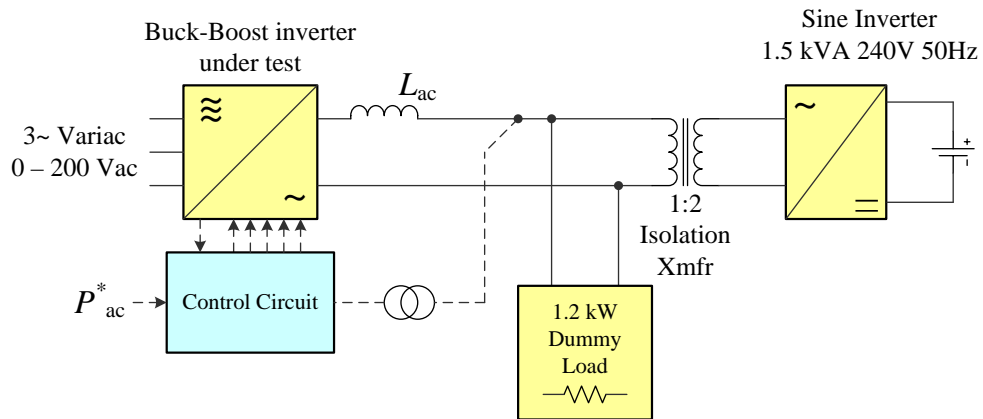


Figure 9. Experimental setup diagram.

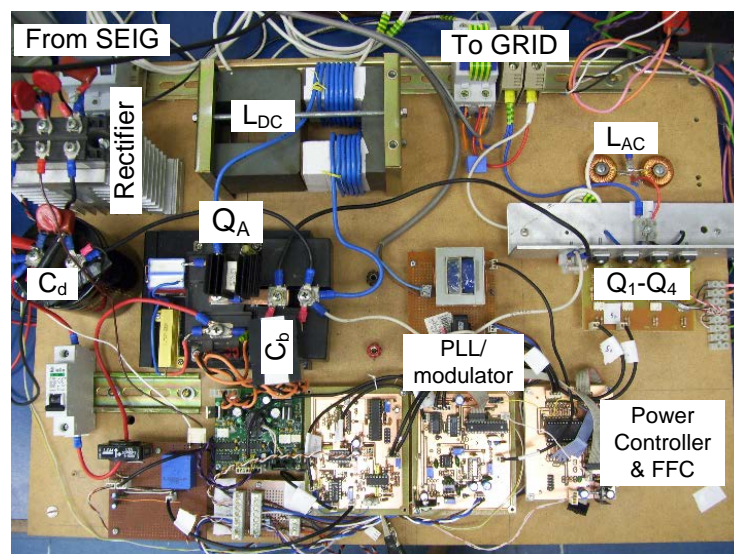


Figure 10. Photograph of inverter prototype.

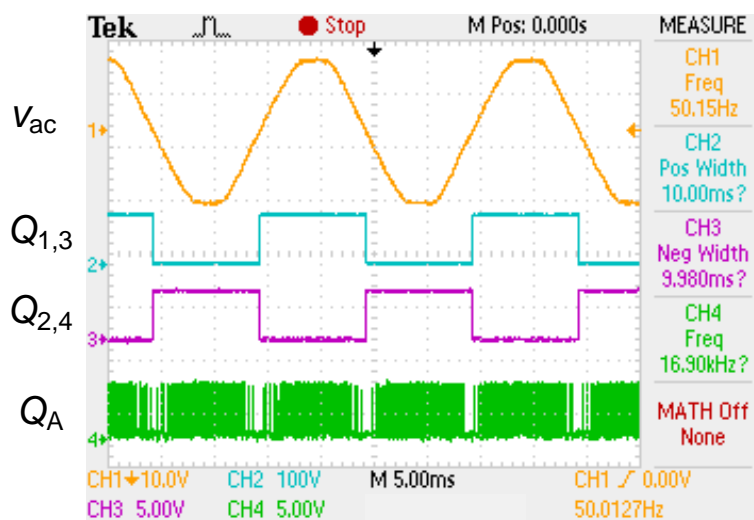


Figure 11. Measured grid voltage and gate signals generated by control circuit.

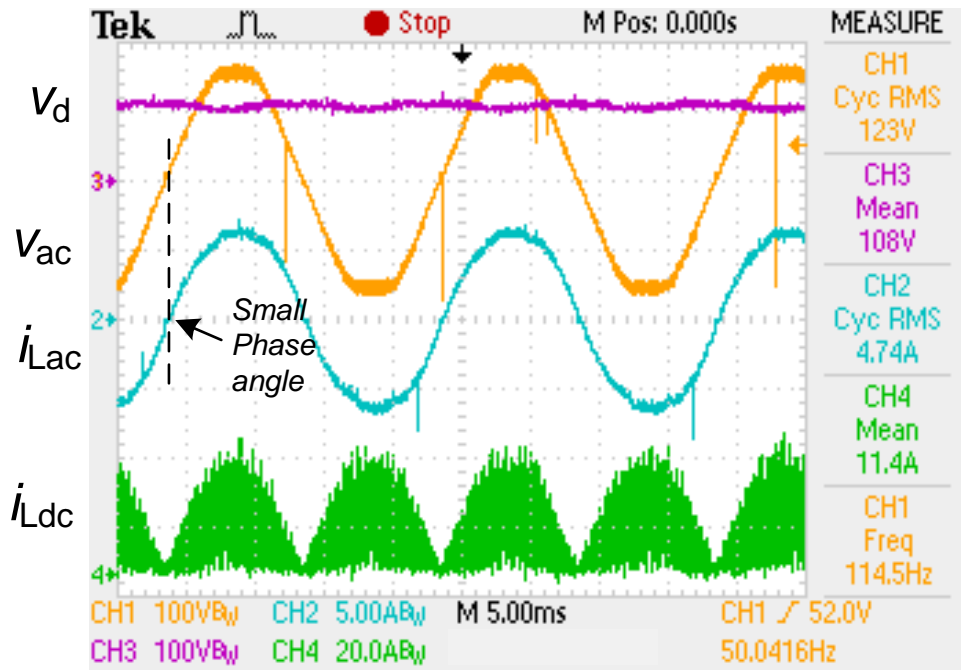


Figure 12. Measured voltage and current waveforms of buck-boost inverter.

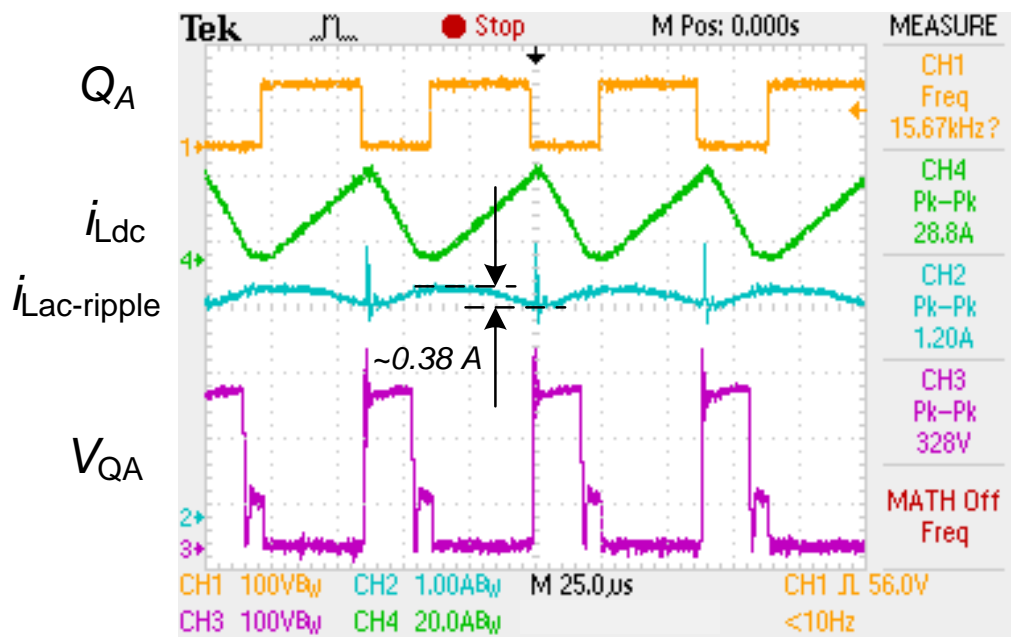


Figure 13. Detailed waveforms of buck-boost inverter..

Low order frequency spectrum of inverter output current was also measured to reveal waveform quality. Frequency spectrum of output current depicted in Figure 14 shows total harmonic distortion and individual distortion which are well below 5%. Thus, it complies with most Total Harmonic Distortion (THD) limitation recommended by most power quality standards.



Figure 14. Measured frequency spectrum of inverter output current.

Conclusions

This paper has presented detailed analysis and design of the buck-boost inverter for wide input voltage application. Inverter parameters were obtained using both analytical and graphical methods which considers power quality of the inverter. Experimental results have been obtained using a scaled-down hardware prototype with results showing a strong correlation with simulations. A low cost microcontroller was sufficient to implement control circuit without compromising quality. Simulation result shows strong conformity to the converter design criteria. However, converter waveform test shows slight deviation from its design criteria. Test results showed ripple on output current is 3.25%. In term of waveform distortion, the THD of output current was less than 5% over a wide range of loads.

References

- [1] L. Wang, H. W. Chen, and D.J. Lee, "Implementation of a DSP-based power converter for a wind induction generator," Paper presented at the *Power and Energy Society General Meeting - Conversion and Delivery of Electrical Energy in the 21st Century*, Pittsburgh, PA, United States of America, 2008.
- [2] A. Macready, and C. Coates, "Low cost wind turbine controller," Paper presented at the *Australasian University Power Engineering Conference*, Perth, Western Australia, Australia, 2007.
- [3] R.M. Hilloowala, and A.M. Sharaf, "A utility interactive wind energy conversion scheme with an asynchronous DC link using a supplementary control loop," *IEEE Transactions on Energy Conversion*, Vol. 9, pp. 558–563, 1994.
- [4] R. Pena, R. Cardenas, R. Blasco, G. Asher, and J. Clare, "A cage induction generator using back to back PWM converters for variable speed grid connected wind energy

- system,” Paper presented at the *27th Annual Conference of Industrial Electronics Society*, Denver, Colorado, United States of America, 2001.
- [5] R.Q. Machado, J.A. Pomilio, and E.G. Marra, “Electronically controlled bi-directional connection of induction generator with a single-phase grid,” Paper presented at the *27th Annual Conference of Industrial Electronics Society*, Denver, Colorado, United States of America, 2001.
 - [6] A. Masaoud, H.W. Ping, S. Mekhilef, and H.O. Belkamel, “A new five-level single-phase inverter employing a space vector current control,” *Electric Power Components and Systems*, Vol. 42, No. 11, pp. 1121–1130, 2014.
 - [7] A. Masaoud, H.W. Ping, S. Mekhilef, and A. Taallah, “Novel configuration for multilevel DC-link three-phase five-level inverter,” *IET Power Electronics*, Vol. 7, No. 12, pp. 3052–3061, 2014.
 - [8] Md.M. Hasan, S. Mekhilef, and M. Ahmed, “Three-phase hybrid multilevel inverter with less power electronic components using space vector modulation,” *IET Power Electronics*, Vol. 7, No. 5, pp. 1256–1265, 2014.
 - [9] S.G. Kumar, S.A. Rahman, and G. Uma, “Operation of self-excited induction generator through matrix converter,” Paper presented at the *Applied Power Electronics Conference and Exposition*, Austin, Texas, United States of America, 2008.
 - [10] S.M. Barakati, M. Kazerani, and X. Chen, “A new wind turbine generation system based on matrix converter,” In: *Power Engineering Society General Meeting*, 2005.
 - [11] F. Kang, and S. Park, “Photovoltaic power interface circuit incorporated with a buck-boost converter and a full-bridge inverter,” *Applied Energy*, Vol. 82, No. 3, pp. 266–283, 2005.
 - [12] M. Nagao, “Power flow of photovoltaic system using buck-boost PWM power inverter,” Paper presented at the *International Conference on Power Electronics and Drive System*, Singapore, Singapore, 1997.